Key Points:
- Two-minute integrated levoglucosan determined from an aircraft platform in winter
- Behavior of levoglucosan and the aerosol mass spectrometer biomass burning marker $\Delta C_2H_4O_2^+$ show some differences
- Based on smoke marker method and literature source ratios, the contribution of residential burning organic carbon ranges from ~30 to 100%

Supporting Information:
- Supporting Information S1

Author Contributions:
Data curation: A. P. Sullivan, H. Guo, J. C. Schroder, P. Campuzano-Jost, J. L. Jimenez, T. Campos, V. Shah, L. Jaeglé, B. H. Lee, F. D. Lopez-Hilfiker, J. A. Thornton, S. S. Brown, R. J. Weber
Formal analysis: A. P. Sullivan
Methodology: A. P. Sullivan
Writing - original draft: A. P. Sullivan
Writing – review & editing: H. Guo, J. C. Schroder, P. Campuzano-Jost, J. L. Jimenez, T. Campos, V. Shah, L. Jaeglé, B. H. Lee, F. D. Lopez-Hilfiker, J. A. Thornton, S. S. Brown, R. J. Weber

Biomass Burning Markers and Residential Burning in the WINTER Aircraft Campaign

A. P. Sullivan[1] , H. Guo[2], J. C. Schroder[3,4] , P. Campuzano-Jost[3,4] , J. L. Jimenez[3,4] , T. Campos[5], V. Shah[6] , L. Jaeglé[6] , B. H. Lee[6] , F. D. Lopez-Hilfiker[6] , J. A. Thornton[6] , S. S. Brown[3,7] , and R. J. Weber[2]

[1]Department of Atmospheric Science, Colorado State University, Fort Collins, CO, USA, [2]School of Earth and Atmospheric Science, Georgia Institute of Technology, Atlanta, GA, USA, [3]Department of Chemistry and Biochemistry, Univeristy of Colorado Boulder, Boulder, CO, USA, [4]Cooperative Institute for Research in Environmental Sciences, University of Colorado Boulder, Boulder, CO, USA, [5]Atmospheric Chemistry Division, National Center for Atmospheric Research, Boulder, CO, USA, [6]Department of Atmospheric Sciences, University of Washington, Seattle, WA, USA, [7]Chemical Sciences Division, Earth System Research Laboratory, National Oceanic and Atmospheric Administration, Boulder, CO, USA

Abstract As part of the WINTER (Wintertime Investigation of Transport, Emissions, and Reactivity) campaign, a Particle-into-Liquid Sampler with a fraction collector was flown aboard the National Center for Atmospheric Research C-130 aircraft. Two-minute integrated liquid samples containing dissolved fine particulate matter (PM_1) species were collected and analyzed off-line for the smoke marker levoglucosan using high-performance anion-exchange chromatography-pulsed amperometric detection to compare levoglucosan with aerosol mass spectrometer (AMS) biomass burning markers and investigate the contribution from residential burning during the study. Levoglucosan was correlated with AMS organic aerosol ($R^2 = 0.49$) and with carbon monoxide (CO; $R^2 = 0.51$) for all flights. Levoglucosan was not correlated with the inorganic smoke marker water-soluble potassium but was correlated with the AMS markers $\Delta C_2H_4O_2^+$ (high resolution, $R^2 = 0.60$) and $\Delta m/z$ 60 (unit mass resolution, $R^2 = 0.61$). However, at low levoglucosan, AMS markers deviated potentially due to interferences from other sources or differences with the species captured by the AMS markers. Analysis of levoglucosan changes relative to carbon monoxide as plumes advected from source regions showed no systematic levoglucosan loss for plumes up to 20 hr old. Based on literature residential burning source ratios and measured levoglucosan, contributions of organic carbon (OC) due to residential burning were estimated. The contribution ranged from ~30 to 100% of the OC, with significant variability depending on the source ratio used; however, the results show that biomass burning was a significant PM_1 OC source across the entire sampling region. A GEOS-Chem model simulation predicted significantly less smoke contribution.

1. Introduction

Biomass burning is a major source of ambient fine particle organic carbon (OC) or organic aerosol (OA) in many regions (Blanchard et al., 2016). Since OA comprises a significant fraction of $PM_{2.5}$ (particulate matter with aerodynamic diameters less than 2.5 μm), often 20 to 90% (Kanakidou et al., 2005), biomass burning smoke can have a large influence on $PM_{2.5}$ concentrations. Contributions are likely to become even more substantial in the future as other anthropogenic sources of $PM_{2.5}$ decrease due to regulation-driven emission reductions (Blanchard et al., 2016) and future burning emissions increase due to changing climate and land use (Hurteau et al., 2014; Pechony & Shindell, 2010). The environmental impacts of biomass burning smoke are substantial and in some cases largely underappreciated. Both black carbon and OC from burning contribute to visibility impairment and affect the global radiation balance (Bond et al., 2013; Streets et al., 2009). On a global scale, biomass burning is likely a major source for brown carbon (Forrister et al., 2015). Light absorption from brown carbon may offset, to some extent, the cooling effect of scattering by the OA component (Feng et al., 2013). Many studies also show that biomass burning smoke is especially toxic (Brook, 2007; Mudway et al., 2005; Torres-Duque et al., 2008; Wegesser et al., 2009) and can significantly contribute to the overall toxicity of $PM_{2.5}$. In metropolitan Atlanta, GA, biomass burning was estimated to contribute 24% to $PM_{2.5}$ water-soluble oxidative potential in the warm seasons and 47% in the cooler

periods (Verma et al., 2014). In this region, oxidative potential was a better predictor of cardiorespiratory emergency department visits than $PM_{2.5}$ mass (Bates et al., 2015).

During spring and summer in the southeastern United States, biomass burning smoke predominately comes from wildfires, agriculture burning, and prescribed burning. However, during cold seasons in the southeast, and especially at higher latitudes (e.g., midwestern and northeastern United States), smoke from residential burning is a significant contributor to $PM_{2.5}$ mass (Jaeckels et al., 2007; Zhang et al., 2010). For example, based on filter samples collected at the St. Louis-Midwest Supersite, the biomass burning contribution to OC was found to be 14% (Jaeckels et al., 2007). Based on data from the Urban Organics Study 2004–2005, 2 to 44% of OC was due to residential burning at the five measurement sites (see http://www.ladco.org/reports/rpo/monitoring/urban_organics_study_integration_final_report_sti_uw.pdf for more information). This has also been found to be true at a number of locations in Europe during winter. For example, it was determined that biomass burning emissions from residential wood burning contributed ~27% in Paris; ~49% in Augsburg, Germany; and ~68% in Zurich to the OC (Crippa et al., 2013; Elsasser et al., 2012; Mohr et al., 2011). To assess and mitigate the impact of biomass burning, determining the contribution of residential burning to the total OC or OA concentration (or $PM_{2.5}$ mass) is vital, particularly during cold seasons when emissions are known to be high.

Smoke marker measurements provide one of the most common methods to estimate contributions of primary particles from residential burning (or any type of primary biomass burning) to the total OC or OA concentration (e.g., Fraser et al., 2003; Rinehart et al., 2006; Schauer et al., 1996; Schauer & Cass, 2000). In this approach, a marker produced as part of the burning emissions is monitored as the plume is transported downwind. If the smoke marker is conserved during transport and the ratio of the smoke marker to the total OC aerosol is known at the source, then a downwind measurement of the smoke marker's concentration can be used to determine the contribution of primary biomass burning to OC or OA. The most common smoke marker used is levoglucosan as it is an anhydrosugar produced from the combustion of cellulose, a major fraction of plant matter (Simoneit et al., 1999). Some studies have reported that levoglucosan may not be conserved due to chemical reactions (Hennigan et al., 2010).

Levoglucosan is typically measured on integrated filter samples collected during ground-based studies with daily resolution and analyzed as monthly composites (e.g., Zheng et al., 2002). This is true for the Midwest studies referenced above as well as most previous studies looking at the impact of residential burning at numerous sites. This is largely because traditional analytical methods, such as gas chromatography-mass spectrometry (GC-MS), require a high concentration of a particular organic species for analysis, preventing the impact of biomass burning via levoglucosan from being routinely explored at higher spatial and temporal scales.

High-performance anion-exchange chromatography with pulsed amperometric detection (HPAEC-PAD) is an alternative highly sensitive method to measure levoglucosan, along with a host of other carbohydrates. PAD is an electrochemical technique where hydroxyl groups are electroanalytically oxidized on the surface of a gold electrode. This approach has the advantage of high chemical specificity associated with chromatographic methods but is a simpler analytical method than GC-MS as no sample derivatization is needed and so levoglucosan can be measured directly in an aqueous sample. The technique has been used on samples for biomass burning source apportionment and biomass burning emission characterization studies (Engling et al., 2006; Gao et al., 2003; Gorin et al., 2006; Puxbaum et al., 2007; Sullivan et al., 2008; Sullivan, Frank, Kenski, & Collett, 2011; Sullivan, Frank, Onstad, et al., 2011). Recently, the technique has been used in an aircraft study to explore biomass burning smoke at a high time resolution (~2 min) by analyzing off-line samples collected by a Particle-into-Liquid Sampler (PILS) and fraction collector system. The data were used to determine biomass burning source characteristics from prescribed burning activities taking place in South Carolina (Sullivan et al., 2014).

Biomass burning markers ($\Delta C_2H_4O_2^+$, high resolution and $\Delta m/z$ 60, unit mass resolution) have also been determined from aerosol mass spectrometer (AMS) measurements (Aiken et al., 2009; Cubison et al., 2011). These markers are also useful for identifying OA factors from biomass burning aerosol based on a positive matrix factorization of AMS spectra. Biomass burning OA factors are often reported in the literature based on such analyses.

Here we report levoglucosan data from a PILS and fraction collector system with off-line analysis by HPAEC-PAD to provide a direct comparison with AMS biomass burning markers with high temporal resolution. We also use the levoglucosan data to explore the spatial and temporal contribution of residential burning in the study region. Data are from the Wintertime Investigation of Transport, Emissions, and Reactivity (WINTER) campaign, an aircraft-based study aimed at examining daytime and nighttime winter chemistry in the northern and eastern United States, a region heavily impacted by residential burning in the cold season.

2. Methods

2.1. The Airborne Mission

The WINTER campaign was a multi-investigator study conducted aboard the National Center for Atmospheric Research (NCAR) C-130 aircraft. The C-130 was operated out of NASA (National Air and Space Administration) Langley Research Center in Hampton, VA from 1 February 2015 to 15 March 2015. A suite of instruments was deployed for measurements of aerosol and trace gas composition. A total of 13 research flights, 7 daytime (RF01, RF02, RF03, RF04, RF11, RF12, and RF13), and 6 nighttime (RF05, RF06, RF07, RF08, RF09, and RF10) were mainly conducted over the northern and eastern United States and focused on investigating sources, transport, mixing, and chemical transformation of wintertime emissions. A map of the flight paths is shown in Figure 9 as part of the discussion presented in section 3.5.

2.2. Particle Collection

During the study, two PILS systems were deployed. A PILS continuously collects ambient particles into purified water, providing a liquid sample for analysis (Orsini et al., 2003). Each PILS instrument sampled from a submicron aerosol inlet (Craig, Moharreri, Schanot, et al., 2013; Craig, Schanot, Moharreri, et al., 2013; Craig et al., 2014; Moharreri et al., 2014). Following each submicron aerosol inlet was a nonrotating MOUDI impactor with a 50% transmission efficiency of 1 μm (aerodynamic diameter) at 1 atmosphere ambient pressure (Marple et al., 1991). The flow rate through the inlet and MOUDI was approximately 15 LPM for each PILS. Upstream of both PILS were two honeycomb denuders coated with sodium carbonate and phosphoric acid to remove inorganic gases to limit possible positive artifacts from dissolving in the PILS collection liquid. The first PILS (PILS1) was connected to two Metrohm ion chromatographs to provide online inorganic ion concentrations every 3 min (Guo et al., 2016). The second PILS (PILS2), which is the focus of this paper, was attached to a Bretchel fraction collector system (Sorooshian et al., 2006) to provide liquid samples for additional off-line analysis. The uncertainty in the PILS measurements was approximately 10%.

PILS2 was set up in a manner similar to that of Sullivan et al. (2014) with minor modifications to the liquid flow rates as PILS2 was coupled to only a fraction collector (i.e., no total organic carbon analyzer) during the WINTER study. The liquid flow rate over the impactor, controlled by a peristaltic pump, was 0.72 ml/min. The liquid sample obtained from the PILS was pushed into the fraction collector vials at a flow rate of 0.65 ml/min for collection of ~1.2 ml of liquid sample per vial.

The Bretchel fraction collector system holds 72 1.5-ml polypropylene vials (Microsolv Technology Corporation, Leland, NC) per carousel. Vials were used as supplied by the manufacturer and were fitted with preslit caps (Microsolv Technology Corporation). The fraction collector program, which was manually started after takeoff, was set to allow continuous collection of 2-min integrated samples (vial fill time). Vial carousels were preloaded before flight. Consecutive carousels were manually switched out as they were filled during flight. Generally, a set of background samples was taken at the beginning of each carousel used during a particular flight by switching a HEPA filter upstream of the PILS in-line for 10 min. At the completion of each flight, the vials were unloaded from the carousels, recapped with solid caps (Microsolv Technology Corporation), packed in coolers with ice packs, and shipped back to Colorado State University to be stored in a 2 °C cold room until analysis began right after completion of the study.

2.3. Off-Line Analysis

Each fraction collector vial was brought to room temperature and then analyzed for levoglucosan as well as a suite of cations and anions/organic acids. In order to conserve sample and allow for analysis of all species, 300-μl aliquots were transferred to polypropylene vials for levoglucosan analysis followed by cation analysis. The remainder of the sample, contained in its original collection vial, but with a new preslit cap, was used

for anion/organic acid analysis. Only levoglucosan and water-soluble potassium are discussed in this paper, and their analysis is explained in more detail below.

The carbohydrate analysis was performed on a Dionex DX-500 series ion chromatograph with detection via an ED-50/ED-50A electrochemical cell. This cell includes two electrodes: a pH-Ag/AgCl (silver/silver chloride) reference electrode and *standard* gold working electrode. For the separation, a sodium hydroxide gradient and a Dionex CarboPac PA-1 column (4×250 mm) were utilized. The complete run time was 59 min with an injection volume of 100 µl. More details on the method can be found in Sullivan et al. (2014), Sullivan, Frank, Kenski, and Collett (2011), Sullivan, Frank, Onstad, et al. (2011). For the WINTER samples, only levoglucosan could be detected with no interferences. It also did not require background correction. Its limit of detection (LOD) based on a sample collection time of 2 min and air flow rate of 15 LPM was determined to be less than approximately 0.10 ng/m^3 with an uncertainty of ~10%.

Water-soluble potassium was measured using a Dionex ICS-3000 ion chromatograph. A Dionex IonPac CS12A analytical column (3×150 mm) with 20-mM methanesulfonic acid provided by an eluent generator at a flow rate of 0.5 ml/min was used for the separation. The complete run time was 17 min with an injection volume of 50 µl. Unlike levoglucosan, a blank correction was necessary for the water-soluble potassium. Concentrations were corrected by using the average of all background samples collected during a specific flight. The LOD for water-soluble potassium was 1 ng/m^3.

2.4. AMS Measurements

Details of the AMS measurements on the C-130 for the WINTER study can be found in Schroder et al. (2018). Briefly, nonrefractory composition of PM$_1$ was measured with a highly customized high-resolution time-of-flight aerosol mass spectrometer (HR-ToF-AMS, Aerodyne Research Inc.; Canagaratna et al., 2007; DeCarlo et al., 2006; Dunlea et al., 2009). A NCAR High-Performance Instrumented Airborne Platform for Environmental Research (HIAPER) Modular Inlet (HIMIL; Stith et al., 2009) sampled the ambient aerosol at a flow rate of 10 LPM. Following this a pressure-controlled AMS inlet was operated at 325 Torr (Bahreini et al., 2008). In the AMS particles were vaporized on a standard porous tungsten vaporizer at 600 °C and the resulting gases ionized via 70-eV electron impact ionization, which were then analyzed by ToF-MS. The AMS OA data were collected at 1-s native resolution using *fast mode* (Kimmel et al., 2011; Schroder et al., 2018), and it is also reported at a 1-min average for convenience for analysis at lower time resolution. The 1-min averaged data are used here. The LOD for 1 min OA during WINTER was 0.19 µg/sm^3. The accuracy for aircraft AMS organic species is approximately ±38% (2σ; Bahreini et al., 2009).

Focusing specifically on the AMS biomass burning markers, experiments show various carbohydrates and carbohydrate anhydrides, with levoglucosan being the most important, produce a distinctive signal at the $C_2H_4O_2^+$ ion at a mass to charge ratio (m/z) 60 (Aiken et al., 2009). Here the term $C_2H_4O_2^+$ refers to the signal measured at the accurate m/z for this ion determined from high-resolution mass spectra, whereas 60 implies determination of this ion signal from mass spectra of unit resolution. Background interferences (from nonbiomass burning sources) at the specific m/z can be removed. Backgrounds are estimated from prior campaigns with minimal impacts from biomass burning and are estimated at 0.3% of the observed OA concentration (Cubison et al., 2011). This was used for both the $C_2H_4O_2^+$ and m/z 60 data. This results in $\Delta C_2H_4O_2^+$ ($=C_2H_4O_2^+ - 0.3\% * OA$) and $\Delta m/z$ 60 ($=m/z$ 60 $- 0.3\% * OA$). (Note that a new notation is being presented here as it is a more accurate representation of these terms. Moving forward it is suggested this notation be used as it is overall clearer. It should also be noted that the data presented here can still be directly compared to all previous results. However, attention should be paid about whether specific studies subtracted the background contribution [as in $\Delta C_2H_4O_2^+$] or not [as in $C_2H_4O_2^+$], and normalizing all the data sets used for comparison to one correction or the other.) These ion signals are often expressed as the ratios to total OA concentration, and then are denoted as $f\Delta C_2H_4O_2^+$ and $f\Delta 60$. $\Delta C_2H_4O_2^+$ is known to be the better biomass burning tracer, since the higher resolution reduces interference from other OA fragments from unrelated sources that may also be present at m/z 60. The ion $\Delta C_2H_4O_2^+$ comprises about 81–93% of the total signal at $\Delta m/z$ 60 during WINTER (e.g., Figure S18 in Schroder et al., 2018). Therefore, our discussions will focus mainly on the biomass burning marker $\Delta C_2H_4O_2^+$. However, $\Delta m/z$ 60 is also of interest since some widely used AMS variants, such as the Aerosol Chemical Speciation Monitor, can only report unit mass resolution data, and many past published papers use $\Delta m/z$ 60.

2.5. Other Measurements

In the following analysis we focus on characterizing residential burning during WINTER. Other airborne measurements utilized include meteorological data and coordinates provided by the Research Aviation Facility as part of the C-130 instrumentation package (http://data.eol.ucar/master_list/?project= WINTER), 1-Hz carbon monoxide (CO) determined by a vacuum UV (ultraviolet) resonance fluorescence method (Gerbig et al., 1999), and 1-s gas-phase smoke markers were quantified by a high-resolution ToF iodide reagent ion chemical ionization mass spectrometer (Lee et al., 2014; Lopez-Hilfiker et al., 2012, 2016; Slusher et al., 2004). All data, including for the PILS, are reported at 1 atm and 273 K.

2.6. GEOS-Chem Model

We compare the tracer-based estimate of the contribution of residential burning to the estimates of biomass burning contribution predicted from GEOS-Chem, a three-dimensional chemical transport model (www.geos-chem.org). We use GEOS-Chem version v10-01, with meteorological fields from the NASA Global Modeling and Assimilation Office GEOS-5 FP model (Molod et al., 2015; Rienecker et al., 2008). GEOS-Chem is run in a nested-gird configuration over North America (10°–60°N, 60°–130°W) at a resolution of 0.5° latitude × 0.625° longitude in the nested domain (Kim et al., 2015). The boundary conditions are from a 4° × 5° resolution global simulation. Anthropogenic emissions of POA over North America are from the U.S. EPA's (Environmental Protection Agency) 2011 Version 6 Emissions Modeling Platform (https://www.epa.gov/air-emissions-modeling/2011-version-6-air-emissions-modeling-platforms; Travis et al., 2016). Fire emissions are from the GFEDv4 inventory (http://www.globalfiredata.org) and biogenic emissions from the Model of Emissions of Gases and Aerosols from Nature (MEGAN v2.1; Guenther et al., 2012). The model output is sampled along the WINTER flight tracks every minute. Details of GEOS-Chem's transport, mixing, and deposition algorithms are available at http://acmg.seas.harvard.edu/geos/geos_chem_narrative.html.

GEOS-Chem simulates the chemistry of primary (POC) and secondary (SOC) OC aerosols in conjunction with the broader tropospheric gas and aerosol-phase chemistry (Bey et al., 2001; Mao et al., 2010; Parrella et al., 2012). The simulation is based on the empirical parameterization developed by Hodzic and Jimenez (2011) and Kim et al. (2015). The approach has two tracers each for anthropogenic POC and SOC: primary and secondary residential wood burning OC (BBPOC and BBSOC) and primary and secondary OC from all other anthropogenic sources (APOC and ASOC). Both POC and SOC are treated as nonvolatile. Emissions of POC from residential wood burning, vehicles, industries, and power plants are included in the NEI. Residential burning emissions are calculated from national and local surveys, fuel sale, and census data and published emission factors (EPA, 2015). In order to match the AMS observations, the POC emissions used in the model simulation from all sources were reduced by half. We use a simple SOC parameterization based on field measurements in lieu of the traditional parameterizations of SOC formation from specific volatile organic compounds (VOCs). In this parameterization, SOC is formed from the oxidation of a lumped VOC tracer emitted from vehicular and wood burning sources with an emissions ratio with respect to CO of 0.069 and 0.013 g VOC/(g CO), respectively (Kim et al., 2015). The VOC is oxidized by hydroxyl radicals at 1.25×10^{-11} cm^3/(mol· s). Biogenic SOC forms with a yield of 3% and 5% from isoprene and monoterpene oxidation, respectively, at the source. Our focus is only comparing the primary biomass burning contribution determined using the tracer-based method to the model BBPOC.

3. Results and Discussion

In the following analysis, we look at the general variation of levoglucosan with other aerosol and gas-phase species that are also emitted in biomass burning, focusing mainly on OA and CO, to investigate the possibility of biomass burning as a source. To improve the analysis, we split the data into two separate measurement periods. We compare levoglucosan to other smoke markers. Then finally we use the levoglucosan to estimate biomass burning OC concentrations and compare them to GEOS-Chem model predictions that use a residential burning emissions inventory.

3.1. Overview

During the WINTER campaign, the average concentration ± standard deviation for levoglucosan, OA, and CO were 0.049 μg/m^3 ± 0.45 μg/m^3, 1.31 μg/m^3 ± 1.08 μg/m^3, and 147 ppbv ± 31 ppbv, respectively. As an
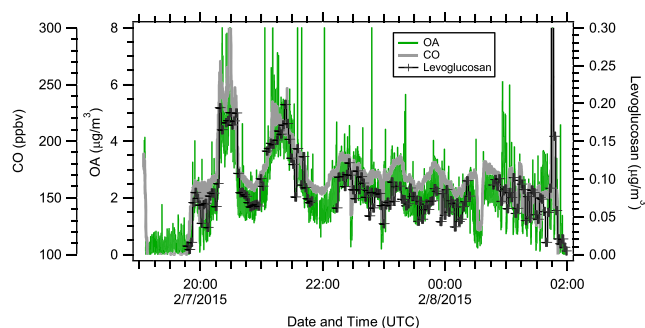
Figure 1. Time series of 1-s CO along with 1-s merged organic aerosol (OA) and levoglucosan from Flight RF03. The sampling altitude for Flight RF03 was ~300 m. Note that since 1-s data are being shown here, the carbon monoxide (CO) and OA concentrations are off-scale for the narrow plume sampled at ~01:45.
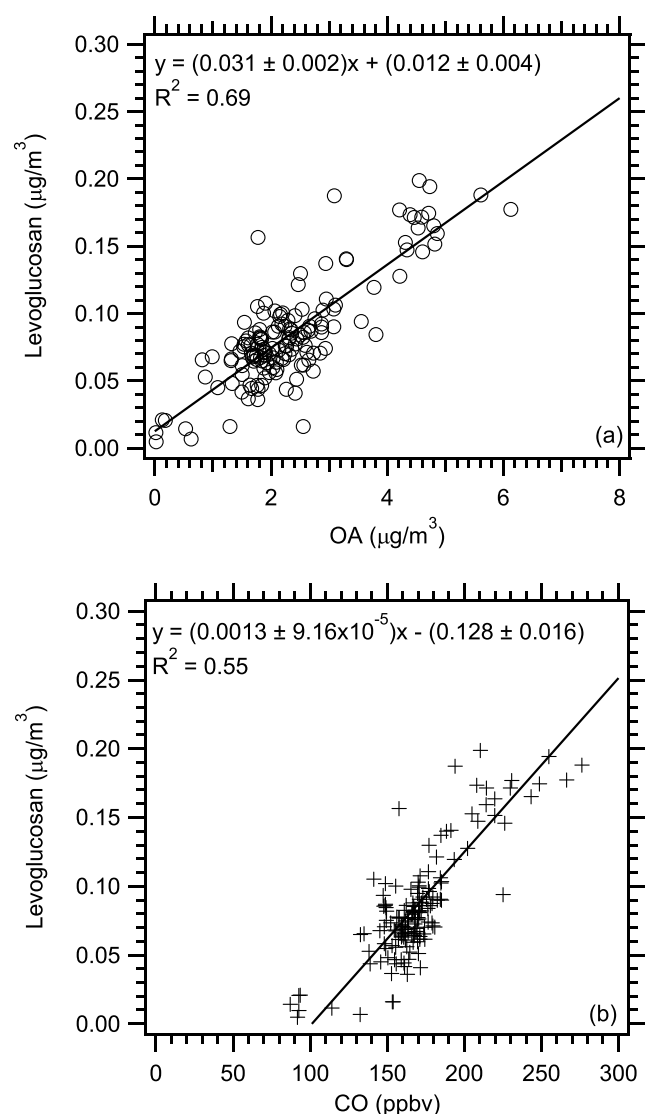

Figure 2. Correlation of levoglucosan versus (a) organic aerosol (OA) and (b) carbon monoxide (CO) for Flight RF03. Uncertainties with the least squares regressions are one standard deviation.

example of the data collected on a flight, the time series for 1 s CO along with 1-s averaged levoglucosan and OA (Figure 1) as well as a comparison of the minute averaged AMS and GEOS-Chem simulated OA (Figure S1 in the supporting information) are shown for Flight RF03. This flight involved following a plume originating from New York City over a period of time (Figure S2). Levoglucosan, OA, and CO concentrations track when sampling both within and out of the plumes, suggesting the importance of biomass burning (indicated by levoglucosan) as one of the sources for both CO and OA throughout this sampling period. However, this should not be overinterpreted, as such correlations in aircraft studies over large polluted regions (such as the northeastern United States) can also be due to entering and exiting polluted air masses where multiple sources contribute. The time series also shows that there was a fairly constant ratio between all three species, which will be discussed in more detail in the next section. The data also demonstrate that the 2-min resolution of the fraction collector is fast enough to capture these plume penetrations. For example, upon examination of the first two plumes in Figure 1, levoglucosan appears to follow some of the finer plume structure within a more broad plume (e.g., the spike and dip observed just before and after 21:30 within the plume sampled from 21:00 to 22:00).

3.2. Levoglucosan Correlation With OA and CO

The correlation between levoglucosan versus OA and CO for Flight RF03 is shown in Figure 2. As expected from the time series, OA ($R^2 = 0.69$) and CO ($R^2 = 0.55$) are correlated with levoglucosan. Similar correlations are also found for the entire data set including all flights (Figures 3a and 3b; levoglucosan versus OA $R^2 = 0.49$ and CO $R^2 = 0.51$) showing the importance of biomass burning as one of the sources for CO and OA throughout the WINTER Study. The levoglucosan versus CO intercept of ~100 ppbv is also consistent with background CO levels. The observation of zero levoglucosan at these CO levels suggests that either the background CO had not been influenced by biomass burning at a detectable level or that the levoglucosan was depleted more rapidly than CO over longer atmospheric processing times of several weeks.

In the following analysis we split the data into two groups for separate analysis. The first series of WINTER Flights (RF01 through RF07) generally had higher levoglucosan average ± standard deviation concentrations (0.076 μg/m^3 ± 0.046 μg/m^3) than the second half of the study (RF08 through RF13, 0.020 μg/m^3 ± 0.015 μg/m^3). Geographical regions sampled and ambient temperature ranges (RF01–RF07 = −17 to 10 °C and RF08–RF13 = −20 to 18 °C) as well as the average temperature below 1,000 m (RF01–RF07 = 3 °C and RF08–RF13 = 7 °C) were similar during both halves of the study. Daytime and nighttime focused flights were included in each half of the study. Figure 4 shows the higher levoglucosan concentrations for all measurement altitudes in the first half of the study. Note that the profile is relatively uniform for the second half of the study (Flights RF08-RF13). But for the first half of the study (Flights RF01-RF07) there is a noticeable increase in concentration at the lower altitudes, suggesting a stronger boundary layer cap on vertical mixing, trapping emissions from residential burning, and leading to higher smoke marker concentrations close to the surface. Similar profiles are seen for OA and CO (Figures 4b and 4c), but less distinct since there are
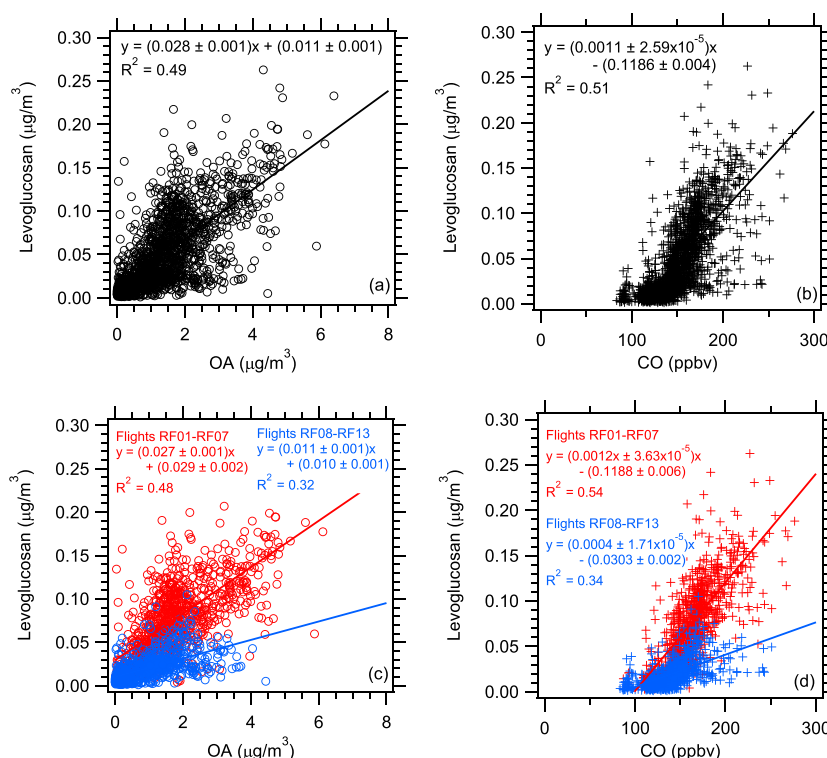
Figure 3. Correlation of levoglucosan versus (a) organic aerosol (OA) for all flights, (b) carbon monoxide (CO) for all flights, (c) OA for all flights with the data segregated into the first (Flights RF01–RF07) and second (Flights RF08–RF13) halves of the study, and (d) CO for all flights with the data segregated into the first (Flights RF01–RF07) and second (Flights RF08–RF13) halves of the study. Uncertainties with the least square regressions are one standard deviation.

additional sources for OA and CO, such as vehicle emissions. This suggests that the biomass burning contribution on the first half of the study was stronger than on the second half.

The scatter plots also reflect the higher levels of levoglucosan. Because there are higher smoke emissions in the first half, higher correlations are expected with OA and CO, as is seen in Figures 3c and 3d (RF01–RF07 levoglucosan versus OA $R^2 = 0.48$ and CO $R^2 = 0.54$; RF08-RF13 levoglucosan versus OA $R^2 = 0.32$ and CO $R^2 = 0.34$).

In summary, we have shown that levoglucosan measured with the PILS with fraction collector system can resolve plumes from biomass burning emissions measured downwind of an urban region when sampling with the NCAR C-130 research aircraft. Comparisons between levoglucosan and OA and CO (R^2 about 0.50) show that about 50% of the variability in OA and CO can be explained by variability in levoglucosan for the overall WINTER data set indicating that this was likely an important source for these species. However, species can also correlate in aircraft studies due to the criss-crossing of clean/mixed/polluted air, so species that are coemitted in populated areas can often be correlated even if they have differences on the detailed sources. Thus, the correlations should not be overinterpreted.

3.3. Relationship Between Levoglucosan and Other Smoke Markers

Other smoke markers were measured during this study, including both aerosol and gas-phase species. Now that we have established
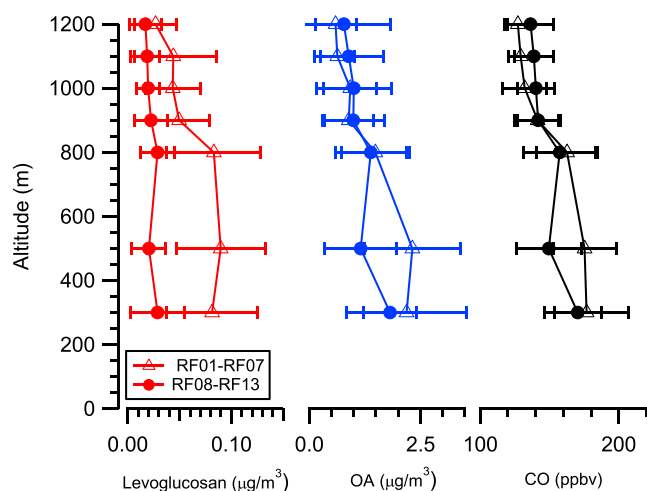

Figure 4. Average altitude profiles of levoglucosan, organic aerosol (OA), and carbon monoxide (CO) for the first (Flights RF01–RF07) and second (Flights RF08–RF13) halves of the study. The error bars are one standard deviation.
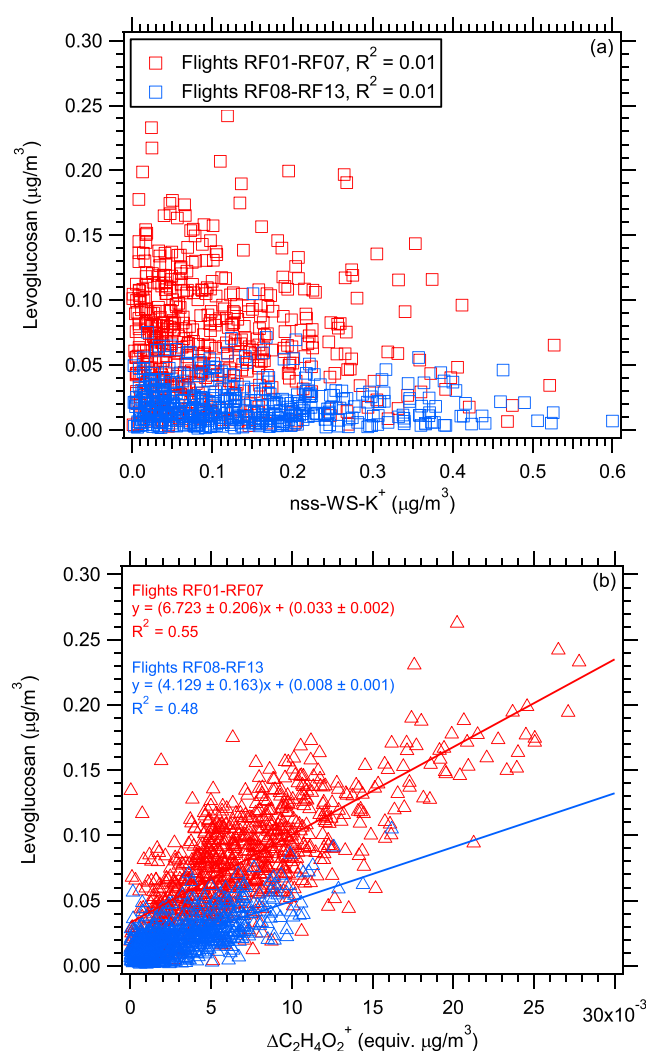
Figure 5. Correlation of levoglucosan versus (a) nss-WS-K$^+$ (non–sea salt–water-soluble potassium) and (b) $\Delta C_2H_4O_2^+$ for all flights with the data segregated into the first (Flights RF01–RF07) and second (Flights RF08–RF13) halves of the study. Uncertainties with the least square regressions are one standard deviation.

that the measured levoglucosan data are consistent with biomass burning substantially impacting particles (OA) and gases (CO), both known to be emitted from biomass burning in general, we compare other more specific smoke markers to levoglucosan.

3.3.1. Aerosol-Phase Smoke Markers

Water-soluble potassium and AMS-measured $\Delta C_2H_4O_2^+$ and $\Delta m/z$ 60 are commonly used aerosol-phase smoke markers. Figure 5a shows that there is no relationship between levoglucosan and nss-WS-K$^+$ (non–sea salt-water-soluble potassium). (Note that nss-WS-K$^+$ was determined from total water-soluble potassium minus water-soluble potassium associated with sea salt. The portion due to sea salt was calculated by multiplying the sodium concentration by the seawater potassium/sodium mass ratio of 0.0359; Seinfeld & Pandis, 1998.) Levoglucosan and nss-WS-K$^+$ for the entire data set (Figure 5a; $R^2 = 0.02$) are not correlated. Similarly, no correlation is observed for either the data segregated into the first or second halves of the study period. There is also no relationship between nss-WS-K$^+$ and OA ($R^2 = 0.04$) or CO ($R^2 = 0.03$; not shown). The lack of correlation between levoglucosan and nss-WS-K$^+$ is likely due to potassium being predominately emitted during the flaming phase of burning, whereas levoglucosan is emitted for all types of burning conditions, for example, smoldering and flaming (Echalar et al., 1995; Lee et al., 2010; Ward et al., 1991). Therefore, a relationship between levoglucosan and potassium is generally only observed under certain burning conditions and fuel type mixtures (Sullivan et al., 2008).

Figure 5b shows the relationship between levoglucosan and AMS $\Delta C_2H_4O_2^+$ and Figure S3 the relationship between levoglucosan and $\Delta m/z$ 60. Also, note that in the main text, high-resolution data from the fragment ion $\Delta C_2H_4O_2^+$ will be shown and the analysis is repeated in the supporting information using unit mass resolution data for $\Delta m/z$ 60. Unlike potassium, $\Delta C_2H_4O_2^+$ and $\Delta m/z$ 60 are correlated with levoglucosan. (Figure 5b, levoglucosan versus $\Delta C_2H_4O_2^+$ for the entire data set $R^2 = 0.60$, Flights RF01–RF07 $R^2 = 0.55$, and Flights RF08-RF13 $R^2 = 0.48$; Figure S3, levoglucosan versus $\Delta m/z$ 60 for the entire data set $R^2 = 0.61$, Flights RF01–RF07 $R^2 = 0.57$, and Flights RF08-RF13 $R^2 = 0.44$.)

Following the same analysis of levoglucosan, the scatter plots for $\Delta C_2H_4O_2^+$ as well as $\Delta m/z$ 60 versus OA and CO for Flight RF03 and all flights are shown in Figures 6 and S4, respectively. Since $\Delta C_2H_4O_2^+$ is known to be the better tracer, we will only discuss this one explicitly, while documenting the relationships for $\Delta m/z$ 60 that are useful for unit mass resolution instruments. Similar to levoglucosan, $\Delta C_2H_4O_2^+$ is correlated with OA ($R^2 = 0.73$) and CO ($R^2 = 0.66$) for Flight RF03, suggesting both indicate biomass burning as a source and both are useful biomass burning markers. However, there are differences between the associations of levoglucosan and $\Delta C_2H_4O_2^+$ with OA and CO when looking at the relationship of each for the data from all flights ($\Delta C_2H_4O_2^+$ versus OA entire data set $R^2 = 0.60$, Flights RF01–RF07 $R^2 = 0.62$, and Flights RF08–RF13 $R^2 = 0.37$ and CO entire data set $R^2 = 0.48$, Flights RF01–RF07 $R^2 = 0.54$, and Flights RF08–RF13 $R^2 = 0.23$). Generally, $\Delta C_2H_4O_2^+$ is somewhat better correlated with OA compared to levoglucosan for all data and each subgroup of flights. We interpret this higher $\Delta C_2H_4O_2^+$ versus OA correlation being due to the same instrument measuring both species, which is not the case for levoglucosan versus OA or levoglucosan and $\Delta C_2H_4O_2^+$ versus CO. Random variability in operating parameters and instrument responses will lead to more scatter when comparing data from two independent measurements. For the comparisons with CO, the levoglucosan association maintains a much clearer distinction between the two periods of the study compared to the $\Delta C_2H_4O_2^+$ versus CO data. This is also true for the comparison with OA, the separation into
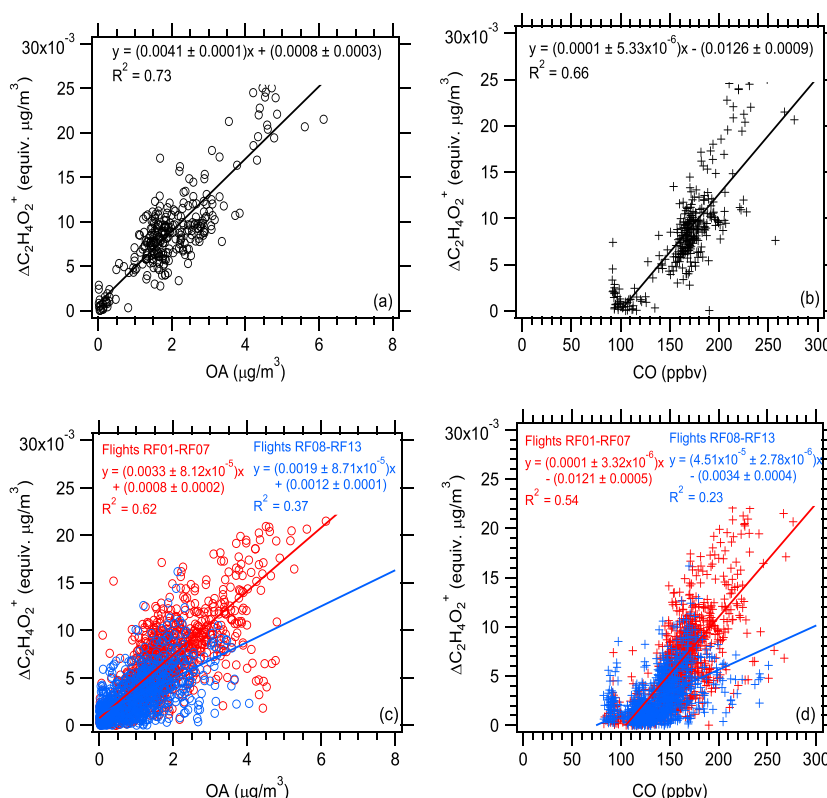
Figure 6. Correlation of $\Delta C_2H_4O_2^+$ versus (a) organic aerosol (OA) and (b) carbon monoxide (CO) for Flight RF03 and (c) OA and (d) CO for all flights with the data segregated into the first (Flights RF01–RF07) and second (Flights RF08–RF13) halves of the study. Uncertainties with the least square regressions are one standard deviation.

the two groups of data is more distinct for levoglucosan (Figure 3). One hypothesis for these differences is that $\Delta C_2H_4O_2^+$ may not be as unique a biomass burning marker as levoglucosan, as ion chromatographic separation may be more chemically selective than a signal at a specific m/z. It is also known that $\Delta C_2H_4O_2^+$ includes contributions from a variety of structurally similar molecules to levoglucosan co-emitted from biomass burning (Aiken et al., 2009; Lee et al., 2010; Mohr et al., 2009), which may add to some of the differences. Thus $\Delta C_2H_4O_2^+$ could have slightly different properties since it includes multiple species and not just levoglucosan (Aiken et al., 2010), and the emission ratios of all species detected as $\Delta C_2H_4O_2^+$ versus levoglucosan may vary with the fuel type and fire conditions. $\Delta C_2H_4O_2^+$ may also be contributed by non biomass burning sources (Cubison et al., 2011; Fortenberry et al., 2018).

3.3.2. Gas-Phase Smoke Markers

A number of gas-phase smoke markers, including HNCO, HCN, $C_2H_4O_2$, $C_3H_6O_2$, $C_4H_6O_2$, $C_5H_5NO_4$, and $C_5H_8O_3$, were also measured as part of the WINTER Study. These species are reported as empirical formulas as their chemical ionization mass spectrometer-measured signal maybe a combination of different isomers (Lee et al., 2014). HNCO and HCN are common gas-phase smoke markers and have been measured in a number of recent studies (e.g., (Roberts et al., 2010, 2011; Simpson et al., 2011)). The other measured gas-phase smoke markers are less well-known, but have also been found to be emitted during biomass burning and are often strongly correlated with HNCO and HCN (e.g., (Christian et al., 2003; Karl et al., 2007)). Just considering RF03, which was highly influenced by biomass burning, a comparison of levoglucosan versus all these gas-phase smoke markers (Figure S5) show that a correlation ($R^2 > 0.60$) is observed between levoglucosan versus $C_2H_4O_2$, $C_3H_6O_2$, and $C_4H_6O_2$. This is also the case for CO, $\Delta C_2H_4O_2^+$, and $\Delta m/z$ 60 versus these smoke markers for RF03 (not shown). The other gas-phase smoke markers were not correlated well with levoglucosan, CO, $\Delta C_2H_4O_2^+$, and $\Delta m/z$ 60. For the entire WINTER data set (Figure S6) only a minor correlation was seen between levoglucosan versus $C_2H_4O_2$, $C_3H_6O_2$, and $C_4H_6O_2$ and there was no strong difference in correlations between the first and second halves of the study. This is likely due to the gas-
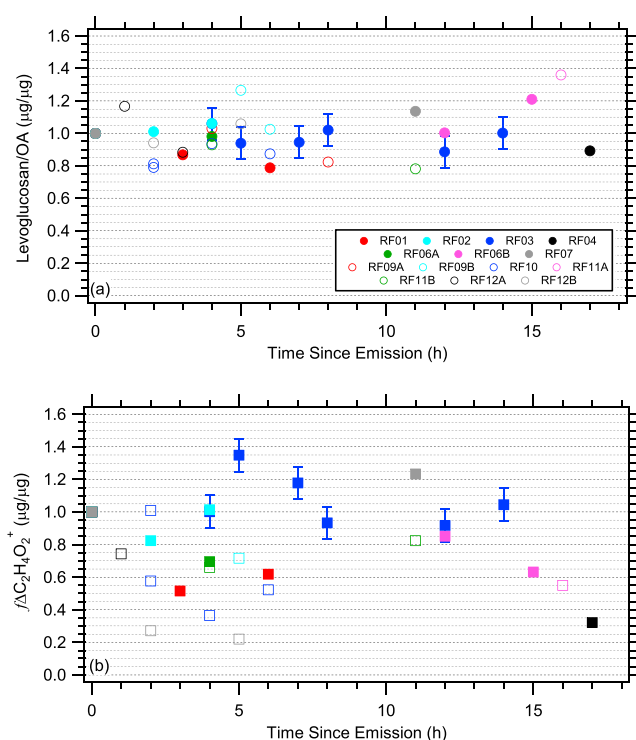
Figure 7. (a) Levoglucosan/OA and (b) $f\Delta C_2H_4O_2^+$ ($\Delta C_2H_4O_2^+$/OA) as a function of time since emission for all flights with the data segregated by flight. For each flight the ratio was normalized by the value at time zero. The uncertainty in the ratios is ~10%.

phase markers having less source specificity as multiple compounds can contribute to each species. (both of these observations were also found in the comparison of the entire data set for CO, $\Delta C_2H_4O_2^+$, and $\Delta m/z$ 60 versus the gas-phase smoke markers, although not shown). Observed differences in the relationship between examining just RF03 and the entire data set also points out that differences in atmospheric lifetimes must be considered when comparing aerosol and gas-phase smoke markers when sampling broad plumes downwind of the source as was often encountered during this study. Thus, aerosol-phase biomass burning smoke markers, such as levoglucosan, may be better than these gas-phase tracers for investigating biomass burning contributions to aerosol mass.

3.4. Stability of Smoke Markers With Plume Age

We now investigate evolution of identified biomass burning plumes as advected away from the source regions to assess the stability of levoglucosan and the AMS smoke markers as the plumes dilute over time. To account for dilution, we normalize the various smoke markers. Since AMS smoke markers are often reported normalized to OA mass ($\Delta C_2H_4O_2^+$/OA and $\Delta m/z$ 60/OA, which are referred to as $f\Delta C_2H_4O_2^+$ and $f\Delta 60$, respectively), a similar analysis is performed here. In addition, the data are normalized to ΔCO, which is a more common practice, where here a hemispheric background of 100 ppbv, based on the intercept of Figure 3b, was used in all cases. Concentrations of the smoke markers outside the plumes are assumed to be 0 (e.g., we plot levoglucosan/ΔCO and $\Delta C_2H_4O_2^+$/ΔCO). Below it will be shown that $f\Delta C_2H_4O_2^+$ and $f\Delta 60$ results are largely similar to the ones with normalization to ΔCO.

From the WINTER data set, biomass burning plumes sampled from the same source, at different distances from the source, were identified for an analysis of the evolution of smoke parameters in plumes as they aged. Figures 7 and 8 show ratios of the biomass burning markers to OA and ΔCO as a function of time since emission (or estimated plume age), respectively. Time since emission was determined by identifying a time zero (i.e., the source), typically an urban location often associated with an aircraft missed landing approach, and determining the time for a back trajectory (Draxler & Rolph, 2016; Rolph, 2016) from the measurement point to pass back through that source region at time zero. The measurement point had to correspond to a fraction collector vial sample. The corresponding higher time resolution data within the plume (OA and CO) were averaged to the vial sample time and then used to calculate the various ratios. The altitude of the measurement point was used in calculating the back trajectory. Analysis was limited to nontransit portions of a flight. In some flights two different specific plumes were identified, in which case they are labeled as A and B.

For each plume, the ratios were normalized to the values at time zero. The various ratios of biomass burning tracer to OA or ΔCO versus time since emissions were also fit with a line determined by linear regression to the nonnormalized data. As a further indicator of change, the percent difference of the various ratios from the start (smallest time) and end (largest time) points for each plume identified are shown in Tables S1–S3 in the supporting information.

For levoglucosan/OA, there is little scatter observed in the data. The absolute value of the percent change in ratio for a specific plume from the start to end data points in most cases was less than 10% (Table S1a). CO would be expected to be more stable than OA if, for example, SOA (secondary OA) formation were occurring with emission time (which is a major effect during WINTER; Schroder et al., 2018) or OA was lost with age due to evaporation of more voltaile components, so normalization by CO should provide a better analysis. Levoglucosan/ΔCO had the same general pattern as levoglucosan/OA as a function of time since emission (Figure 8a) and the absolute value of the percent change in the ratio from the start to end data are similarly low as to those observed for the

Figure 8. (a) Levoglucosan/ΔCO and (b) $\Delta C_2H_4O_2^+$/ΔCO as a function of time since emission for all flights with the data segregated by flight. For each flight the ratio was normalized by the value at time zero. The uncertainty in the ratios is ~10%.

levoglucosan/OA (Table S1b). These data suggest that for the conditions of this study, levoglucosan is not significantly lost due to chemical reaction on times of up to approximately 20 hr.

$f\Delta C_2H_4O_2^+$ as a function of time since emission is shown in Figure 7b. There is more scatter in the $f\Delta C_2H_4O_2^+$ data versus emission time compared to levoglucosan. Also, there might be a larger absolute value of the percent change in the ratio from the start to end data point (Table S2a). But this pattern appears to be even more pronounced when examining $\Delta C_2H_4O_2^+$/ΔCO as a function of emission time (Figure 8b and Table S2b). Some of these differences might result from changes in this AMS smoke marker being more sensitive to changes in background OA concentration. The greater scatter in the evolution of this AMS smoke marker may also be due to interferences from other nonsmoke ions at this m/z. This interference would be more evident as the concentrations of the smoke marker ions get smaller, such as in dilute plumes.

The same trends are observed for $\Delta m/z$ 60 as shown in Figure S7 and Table S3. Previous studies examining the stability of $\Delta m/z$ 60 have been conducted using laboratory burns usually in combination with photo-oxidation experiments (Hennigan et al., 2010, 2011; Heringa et al., 2011; Ortega et al., 2013). These experiments have examined $f\Delta$60 as a function of hydroxyl radical exposure, photochemical age, or time since lights on. This in combination with nonambient data prevents a direct comparison from being made.

3.5. Estimation of the Contribution of Residential Burning to OC

Figure 9 provides maps of the levoglucosan concentration across the sampling region. From these data the contribution of residential burning to PM$_1$ OA (in this case OC mass, OC) during WINTER can be estimated. To estimate this impact, we use a tracer method. This method is one of the most common and has been employed in a number of previous studies (e.g., Fraser et al., 2003; Rinehart et al., 2006; Schauer et al., 1996; Schauer & Cass, 2000). Most burning in this study is expected to be from residential burning given the location (midwestern and northeastern United States) and time of year (cold season). The percentage contribution of primary residential biomass burning to total OC is estimated by dividing the measured levoglucosan/OC ratio of an ambient sample by the levoglucosan/OC ratio from a residential burning source profile and multiplying by 100. Given the sampling region for WINTER, two possible source levoglucosan/OC ratios could be used, one for residential burning involving northeastern fuels (0.045 ± 0.017 μg C/μg C) and one for midwestern fuels (0.070 ± 0.045 μg C/μg C). These values were determined by averaging all the source profiles from each specific region presented in Fine et al. (2001, 2004) and converting them to a carbon mass basis. The difference in the ratios comes from the different fuels typically burned in the two regions. The ambient levoglucosan concentrations are from the PILS with fraction collector system off-line measurements. Ambient OC concentrations are from AMS OA data; OC was determined by converting the measured OA to OC using the AMS OA/OC ratios measured for each data point.

This tracer method approach has a number of limitations. It can be affected by variations of the emission ratio not captured by the limited literature tests used here. It also ignores the evolution of OA as it ages; hence, it is referred to as an estimate of the primary aerosol residential biomass burning fraction, assuming that the primary OC does not change with aging. It also assumes that levoglucosan is stable on the time scales of the plume ages investigated here; from the analysis above, this is a reasonable assumption. In any case, estimates of the biomass burning fraction to OC for more aged plumes are more uncertain. This analysis will underestimate biomass burning conditions if there is either a loss of levoglucosan due to photochemical aging (Hennigan et al., 2010) or OC increases relative to levoglucosan due to SOA formation (from biomass burning precursors) during aging. Overestimation would occur if levoglucosan was formed (not likely) as levoglucosan is not known to be a secondary product, if OC was lost relative to levoglucosan,
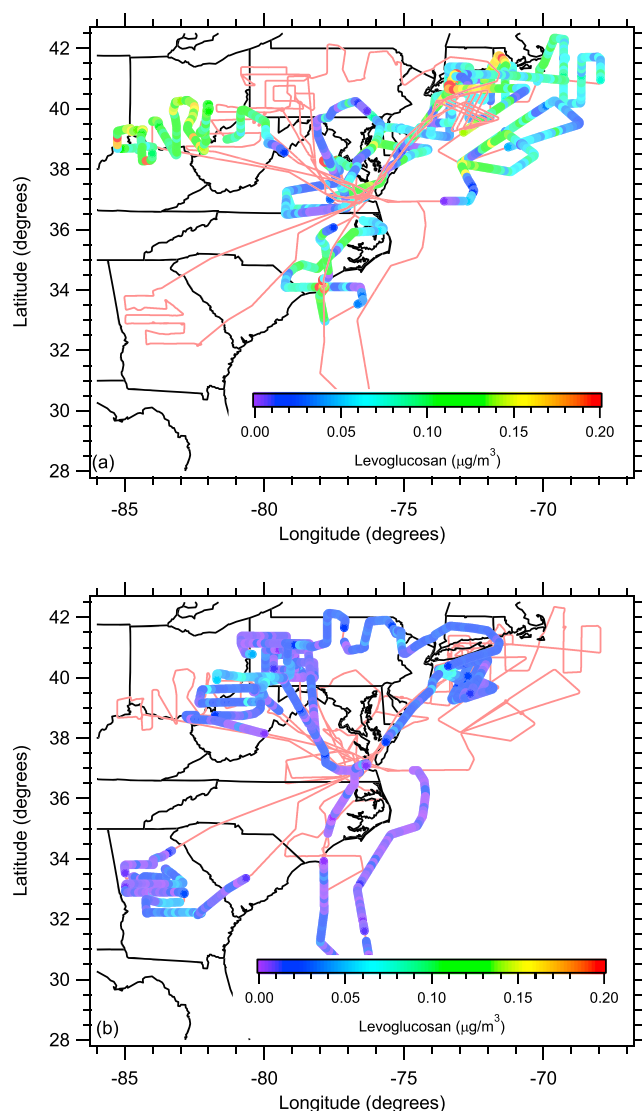
Figure 9. Map showing the levoglucosan concentration for the (a) first (Flights RF01–RF07) and (b) second (Flights RF08–RF13) halves of the study.

such as by evaporation of OC, or if the emission ratios used here were too low compared to the real emissions during WINTER.

Figures S8 and S9 provide maps of the contribution of OC due to residential burning during WINTER. The maps have been segregated into the two halves of the study and are shown using both sets of source profiles to provide a sense of the possible range in the estimate. When using the source profile for the burning of Northeastern fuels, the average contribution $\pm$ standard deviation of residential biomass burning for the first half of the study is 99% $\pm$ 48% and for the second half of the study 64% $\pm$ 31%. This changes to 43% $\pm$ 25% and 27% $\pm$ 16% for the first and second halves of this study, respectively, when using the source profile for the burning of midwestern fuels. The range of the average values provides an indication of the effect of the assumed source profile; thus, in the first half of the study where the levoglucosan concentrations was higher and more correlated with OA and CO, the estimated range in biomass burning OC to total PM_1 OC is roughly 40 to 100%, in contrast to 30 to 40% in the second half of the study. Although there is significant uncertainty in the tracer method, reflected in the wide range determined in predicted biomass burning OC fraction, this analysis does indicate that for this study, biomass burning OC was ubiquitous, regardless of location or time of day.

As an alternative to using a literature valve for the source ratio, we also explored using the data to provide this ratio. A levoglucosan/OA ratio can be determined by taking the difference of the average of the lowest three points in the altitude profiles for the first half to the second half of the study plotted in Figure 4. Two assumptions are required to use this method: the emission ratio is the same between both halves of the study and the changes in the two halves of the study are dominated by residential burning. The lowest three points are most likely in the boundary layer and where the two halves of study are most different. Finally, to convert to a levoglucosan/OC ratio, the average $\pm$ standard deviation AMS OA/OC ratio for the entire study of 2.17 $\pm$ 0.27 can be applied, providing a levoglucosan/OC ratio of 0.104 μg C/μg C. Figure S10 provides maps of the contribution of residential burning determined using this alternative ratio. The average contribution $\pm$ standard deviation of residential burning for the first half of the study is 45% $\pm$ 32% and for the second half of the study 19% $\pm$ 16%, fairly similar to the results obtained using the literature source profile for the Midwestern fuels.

Positive matrix factorization analysis was conducted on the AMS data to determine the sources of OA during WINTER. Biomass burning OA was found to be fairly ubiquitous and accounted for 32% of the OA (Schroder et al., 2018). This falls between the average values observed for the first and second halves of the study using the literature source profile for midwestern fuels or using the data to provide the ratio.

The tracer method results can also be compared to GEOS-Chem model simulations in which the contribution of primary and secondary OC due to biomass burning was determined along the flight tracks. From examination of Figure S11 it can be observed that the contribution of residential burning determined by the model is lower than what was determined using the tracer method. The model does, however, capture the broad spatial trends as does the inventory (Figure S12). The model also does produce the difference in the two halves of the study (RF01–RF07 = 25% $\pm$ 12% and RF08–RF13 = 13% $\pm$ 11%) as suggested by the levoglucosan data. There are many factors that could lead to the disagreement between the contribution of residential biomass burning determined between the model and the tracer method, including differences in emissions, transport, and chemical evolution. The evidence from this study suggests that it is largely due

to how the emissions are handled in the model as there is very little agreement between the primary biomass burning OC determined by the model and the measured levoglucosan (Flights RF01–RF07 $R^2 = 0.34$ and Flights RF08–RF13 $R^2 = 0.25$; Figure S13). In addition, the comparison of the model and tracer estimates of residential biomass burning contributions to OC is improved if the POC emissions in the model simulation (see section 2.6) are not reduced by half (RF01–RF07 = 32% ± 14% and RF08–RF13 = 18% ± 14%, not shown) or if the primary and secondary residential burning determined by the model are summed (RF01–RF07 = 31% ± 11% and RF08–RF13 = 23% ± 10%; Figure S14). Then the model results are more similar to those determined by the tracer method using the source profile for residential burning involving midwestern fuels (Figure S14 vs. Figure S9). Overall, the wide range of results suggests that more work is still needed in understanding the appropriate source profiles to use. However, the results from all approaches indicate that residential burning is an important fraction of the OC measured during WINTER.

4. Summary

A Particle-into-Liquid Sampler system with a fraction collector was deployed on the C-130 research aircraft during the WINTER campaign in order to collect samples for off-line analysis. The samples were analyzed using HPAEC-PAD to provide a 2-min integrated continuous measurement of the smoke marker levoglucosan in order to explore the contribution of residential burning to PM_1 OC during the study. Comparisons with CO and OA showed that the 2-min time resolution was adequate to detect plumes, and fine-scale plume structure, down to very low levoglucosan concentrations (LOD of at least 0.10 ng/m^3). These data represent only the second set of airborne measurements for levoglucosan and the first from a region highly impacted by residential burning.

Levoglucosan was correlated with OA ($R^2 = 0.49$) and CO ($R^2 = 0.51$) for all flights, suggesting the importance of biomass burning as one of the sources during WINTER. In addition, the data fell into two distinct groups representing the first (Flights RF01–RF07) and second (Flights RF08–RF13) halves of the study. Levoglucosan was not correlated with the inorganic smoke marker water-soluble potassium, likely because it is known that potassium is predominately emitted during only the flaming phase. However, levoglucosan was correlated with the AMS biomass burning markers $\Delta C_2H_4O_2^+$ and $\Delta m/z$ 60 ($\Delta C_2H_4O_2^+$ entire data set $R^2 = 0.60$ and $\Delta m/z$ 60 entire data set $R^2 = 0.61$). The behavior of these species showed small differences when exploring the levoglucosan/OA and $\Delta C_2H_4O_2^+$/OA ratios as a function of time since emission. Levoglucosan showed no systematic evidence of loss relative to OA or CO with time since emission, for emission times up to 20 hr, whereas the AMS smoke markers were less clear. Differences in the behavior of levoglucosan and AMS smoke markers are thought to be due to greater chemical specificity of the levoglucosan measurements, whereas the AMS markers can represent a broader biomass burning marker due to (helpful) contributions of nonlevoglucosan biomass burning markers or alternatively due to (unhelpful) interferences from other nonbiomass burning OA species to $\Delta C_2H_4O_2^+$ that are not captured by the background subtraction applied. This study demonstrates the utility of measurements with high chemical selectivity when quantifying sources.

Estimation of the contribution of OC due to residential burning using a tracer method based on levoglucosan suggested that it was a large and significant source for OC across the entire sampling region during the study, with the contribution ranging from ~30 to 100%. Some of the variability is due to the use of two literature emission factors assumed to represent the range of expected emissions for residential burning in the region. A GEOS-Chem model simulation predicted substantially lower biomass burning contributions (RF01–RF07 = 25% ± 12% and RF08–RF13 = 13% ± 11%) likely due to how the emissions are handled in the model. But the results were spatially consistent with the levoglucosan data and also predicted a difference in residential burning contributions in the first and second halves of the WINTER study.

References

Aiken, A., Salcedo, D., Cubison, M. J., Huffman, J. A., DeCarlo, P. F., Ulbrich, I. M., et al. (2009). Mexico City aerosol analysis during MILAGRO using high resolution aerosol mass spectrometry at the urban supersite (T0)—Part 1: Fine particle composition and organic source apportionment. *Atmospheric Chemistry and Physics*, *9*, 6633–6653.

Aiken, A. C., de Foy, B., Wiedinmyer, C., DeCarlo, P. F., Ulbrich, I. M., Wehrli, M. N., et al. (2010). Mexico city aerosol analysis during MILAGRO using high resolution aerosol mass spectrometry at the urban supersite (T0) – Part 2: Analysis of the biomass burning

contribution and the non-fossil carbon fraction. *Atmospheric Chemistry and Physics*, 10, 5315–5341. https://doi.org/10.5194/acp-10-5315-2010

Bahreini, R., Dunlea, E. J., Matthew, B. M., Simons, C., Docherty, K. S., DeCarlo, P. F., et al. (2008). Design and operation of a pressure-controlled inlet for airborne sampling with an aerodynamic aerosol lens. *Aerosol Science and Technology*, 42(6), 465–471. https://doi.org/10.1080/02786820802178514

Bahreini, R., Ervens, B., Middlebrook, A. M., Warneke, C., de Gouw, J. A., DeCarlo, P. F., et al. (2009). Organic aerosol formation in urban and industrial plumes near Houston and Dallas, Texas. *Journal of Geophysical Research*, 114, D00F16. https://doi.org/10.1029/2008JD011493

Bates, J. T., Weber, R. J., Abrams, J., Verma, V., Fang, T., Klein, M., et al. (2015). Reactive oxygen species generation linked to sources of atmospheric particulate matter and cardiorespiratory effects. *Environmental Science & Technology*, 49(22), 13,605–13,612. https://doi.org/10.1021/acs.est.5b02967

Bey, I., Jacob, D. J., Yantosca, R. M., Logan, J. A., Field, B. D., Fiore, A. M., et al. (2001). Global modeling of tropospheric chemistry with assimilated meteorology: Model description and evaluation. *Journal of Geophysical Research*, 106(D19), 23,073–23,095. https://doi.org/10.1029/2001JD000807

Blanchard, C. L., Hidy, G. M., Shaw, S., Baumann, K., & Edgerton, E. S. (2016). Effects of emission reductions on organic aerosol in the southeastern United States. *Atmospheric Chemistry and Physics*, 16(1), 215–238. https://doi.org/10.5194/acp-16-215-2016

Bond, T. C., Doherty, S. J., Fahey, D. W., Forster, P. M., Berntsen, T., DeAngelo, B. J., et al. (2013). Bounding the role of black carbon in the climate system: A scientific assessment. *Journal of Geophysical Research: Atmospheres*, 118, 5380–5552. https://doi.org/10.1002/jgrd.50171

Brook, R. D. (2007). Why physicians who treat hypertension should know more about air pollution. *The Journal of Clinical Hypertension*, 9(8), 629–635. https://doi.org/10.1111/j.1524-6175.2007.07187.x

Canagaratna, M. R., Jayne, J. T., Jimenez, J. L., Allan, J. D., Alfarra, M. R., Zhang, Q., et al. (2007). Chemical and microphysical characterization of ambient aerosols with the aerodyne aerosol mass spectrometer. *Mass Spectrometry Reviews*, 26(2), 185–222. https://doi.org/10.1002/mas.20115

Christian, T. J., Kleiss, B., Yokelson, R. J., Holzinger, R., Crutzen, P. J., Hao, W. M., et al. (2003). Comprehensive laboratory measurements of biomass-burning emissions: 1. Emissions from Indonesian, African, and other fuels. *Journal of Geophysical Research*, 108(D23), 4719. https://doi.org/10.1029/2003JD003704

Craig, L., Moharreri, A., Rogers, D. C., Anderson, B., & Dhaniyala, S. (2014). Aircraft-based aerosol sampling in clouds: Performance characterization of flow-restriction aerosol inlets. *Journal of Atmospheric and Oceanic Technology*, 31(11), 2512–2521. https://doi.org/10.1175/jtech-d-14-00022.1

Craig, L., Moharreri, A., Schanot, A., Rogers, D. C., Anderson, B., & Dhaniyala, S. (2013). Characterizations of cloud droplet shatter artifacts in two airborne aerosol inlets. *Aerosol Science and Technology*, 47(6), 662–671. https://doi.org/10.1080/02786826.2013.780648

Craig, L., Schanot, A., Moharreri, A., Rogers, D. C., & Dhaniyala, S. (2013). Design and sampling characteristics of a new airborne aerosol inlet for aerosol measurements in clouds. *Journal of Atmospheric and Oceanic Technology*, 30(6), 1123–1135. https://doi.org/10.1175/jtech-d-12-00168.1

Crippa, M., DeCarlo, P. F., Slowik, J. G., Mohr, C., Heringa, M. F., Chirico, R., et al. (2013). Wintertime aerosol chemical composition and source apportionment of the organic fraction in the metropolitan area of Paris. *Atmospheric Chemistry and Physics*, 13, 961–981. https://doi.org/10.5194/acp-13-961-2013

Cubison, M. J., Ortega, A. M., Hayes, P. L., Farmer, D. K., Day, D., Lechner, M. J., et al. (2011). Effects of aging on organic aerosol from open biomass burning smoke in aircraft and laboratory studies. *Atmospheric Chemistry and Physics*, 11(23), 12,049–12,064. https://doi.org/10.5194/acp-11-12049-2011

DeCarlo, P. F., Kimmel, J. R., Trimborn, A., Northway, M. J., Jayne, J. T., Aiken, A. C., et al. (2006). Field-deployable, high-resolution, time-of-flight aerosol mass spectrometer. *Analytical Chemistry*, 78(24), 8281–8289. https://doi.org/10.1021/ac061249n

Draxler, R. R., & Rolph, G. D. (2016). HYSPLIT (HYbrid Single-Particle Lagrangian Integrated Trajectory) model access via NOAA ARL READY website. http://www.arl.noaa.gov/ready/hysplit4.html (last access: 31 August 2016).

Dunlea, E. J., DeCarlo, P. F., Aiken, A. C., Kimmel, J. R., Peltier, R. E., Weber, R. J., et al. (2009). Evolution of Asian aerosols during transpacific transport in INTEX-B. *Atmospheric Chemistry and Physics*, 9, 7257–7287. https://doi.org/10.5194/acp-9-7257-2009

Echalar, F., Gaudichet, A., Cachier, H., & Artaxo, P. (1995). Aerosol emissions by tropical forest and savanna biomass burning: Characteristic trace elements and fluxes. *Geophysical Research Letters*, 22(22), 3039–3042. https://doi.org/10.1029/95GL03170

Elsasser, M., Crippa, M., Orasche, J., DeCarlo, P. F., Oster, M., Pitz, M., et al. (2012). Organic molecular markers and signature from wood combustion particles in winter ambient aerosols: Aerosol mass spectrometer (AMS) and high-time resolved GC-MS measurements in Augsburg, Germany. *Atmospheric Chemistry and Physics*, 12(14), 6113–6128. https://doi.org/10.5194/acp-12-6113-2012

Engling, G., Carrico, C. M., Kreidenweis, S. M., Collett, J. L., Jr., Day, D. E., Malm, W. C., et al. (2006). Determination of levoglucosan in biomass combustion aerosol by high-performance anion-exchange chromatography with pulsed amperometric detection. *Atmospheric Environment*, 40, S299–S311.

EPA (2015). *2011 National Emissions Inventory Version 2 technical support document*. NC: Research Triangle Park.

Feng, Y., Ramanathan, V., & Kotamarthi, V. R. (2013). Brown carbon: A significant atmospheric absorber of solar radiation? *Atmospheric Chemistry and Physics*, 13(17), 8607–8621. https://doi.org/10.5194/acp-13-8607-2013

Fine, P. M., Cass, G. R., & Simoneit, B. R. T. (2001). Chemical characterization of Fine particle emissions from fireplace combustion of woods grown in the northeastern United States. *Environmental Science & Technology*, 35(13), 2665–2675. https://doi.org/10.1021/es001466k

Fine, P. M., Cass, G. R., & Simoneit, B. R. T. (2004). Chemical characterization of fine particle emissions from the fireplace combustion of wood types grown in the midwestern and western United States. *Environmental Engineering Science*, 21(3), 387–409. https://doi.org/10.1089/109287504323067021

Forrister, H., Liu, J., Scheuer, E., Dibb, J., Ziemba, L., Thornhill, K. L., et al. (2015). Evolution of brown carbon in wildfire plumes. *Geophysical Research Letters*, 42, 4623–4630. https://doi.org/10.1002/2015GL063897

Fortenberry, C. F., Walker, M. J., Zhang, Y., Mitroo, D., Brune, W. H., & Williams, B. J. (2018). Bulk and molecular-level characterization of laboratory-aged biomass burning organic aerosol from oak leaf and heartwood fuels. *Atmospheric Chemistry and Physics*, 18(3), 2199–2224. https://doi.org/10.5194/acp-18-2199-2018

Fraser, M. P., Yue, Z. W., & Buzcu, B. (2003). Source appointment of fine particulate matter in Houston, TX, using organic molecular markers. *Atmospheric Environment*, 37(15), 2117–2123. https://doi.org/10.1016/S1352-2310(03)00075-X

Gao, S., Hegg, D. A., Hobbs, P. V., Kirchstetter, T. W., Magi, B. I., & Sadilek, M. (2003). Water-soluble organic components in aerosols associated with savanna fires in southern Africa: Identification, evolution, and distribution. *Journal of Geophysical Research*, 108(D13), 8491. https://doi.org/10.1029/2002JD002324

Gerbig, C., Schmitgen, S., Kley, D., Volz-Thomas, A., Dewey, K., & Haaks, D. (1999). An improved fast-response vacuum-UV resonance fluorescence CO instrument. *Journal of Geophysical Research*, *104*(D1), 1699–1704. https://doi.org/10.1029/1998JD100031

Gorin, C. A., Collett, J. L., Jr., & Herckes, P. (2006). Wood smoke contribution to winter aerosol in Fresno, CA. *Journal of the Air & Waste Management Association*, *56*(11), 1584–1590. https://doi.org/10.1080/10473289.2006.10464558

Guenther, A. B., Jiang, X., Heald, C. L., Sakulyanontvittaya, T., Duhl, T., Emmons, L. K., & Wang, X. (2012). The Model of Emissions of Gases and Aerosols from Nature version 2.1 (MEGAN 2.1): an extended and updated framework for modeling biogenic emissions. *Geoscientific Model Development*, *5*, 1471–1491.

Guo, H., Sullivan, A. P., Campuzano-Jost, P., Schroder, J. C., Lopez-Hilfiker, F. D., Dibb, J. E., et al. (2016). Fine particle pH and the partitioning of nitric acid during winter in the northeastern United States. *Journal of Geophysical Research: Atmospheres*, *121*, 355–310. https://doi.org/10.1002/2016JD025311

Hennigan, C. J., Miracolo, M. A., Engelhart, G. J., May, A. A., Presto, A. A., Lee, T., et al. (2011). Chemical and physical transformations of organic aerosol from the photo-oxidation of open biomass burning emission in an environmental chamber. *Atmospheric Chemistry and Physics*, *11*(15), 7669–7686. https://doi.org/10.5194/acp-11-7669-2011

Hennigan, C. J., Sullivan, A. P., Collett, J. L., Jr., & Robinson, A. L. (2010). Levoglucosan stability in biomass burning particles exposed to hydroxyl radicals. *Geophysical Research Letters*, *37*, L09806. https://doi.org/10.1029/2010GL043088

Heringa, M. F., DeCarlo, P. F., Chirico, R., Tritscher, T., Dommen, J., Weingartner, E., et al. (2011). Investigations of primary and secondary particulate matter of different wood combustion appliances with a high-resolution time-of-flight aerosol mass spectrometer. *Atmospheric Chemistry and Physics*, *11*(12), 5945–5957. https://doi.org/10.5194/acp-11-5945-2011

Hodzic, A., & Jimenez, J. L. (2011). Modelling anthropogenically controlled secondary organic aerosols in a megacity: A simplified framework for global and air quality models. *Geoscientific Model Development*, *4*(4), 901–917. https://doi.org/10.5194/gmd-4-901-2011

Hurteau, M. D., Westerling, A. L., Wiedinmyer, C., & Bryant, B. P. (2014). Projected effects of climate and development on California wildfire emissions through 2100. *Environmental Science & Technology*, *48*(4), 2298–2304. https://doi.org/10.1021/es4050133

Jaeckels, J. M., Bae, M. S., & Schauer, J. J. (2007). Positive matrix factorization (PMF) analysis of molecular marker measurements to quantify the sources of organic aerosols. *Environmental Science & Technology*, *41*(16), 5763–5769. https://doi.org/10.1021/es062536b

Kanakidou, M., Seinfeld, J. H., Pandis, S. N., Barnes, I., Dentener, F. J., Facchini, M. C., et al. (2005). Organic aerosol and global climate modelling: A review. *Atmospheric Chemistry and Physics*, *5*(4), 1053–1123. https://doi.org/10.5194/acp-5-1053-2005

Karl, T. G., Christian, T. J., Yokelson, R. J., Artaxo, P., Hao, W. M., & Guenther, A. (2007). The tropical Forest and fire emissions experiment: Method evaluation of volatile organic compound emissions measured by PTR-MS, FTIR, and GC from tropical biomass burning. *Atmospheric Chemistry and Physics*, *7*(22), 5883–5897. https://doi.org/10.5194/acp-7-5883-2007

Kim, P., Jacob, D. J., Fisher, J. A., Travis, K., Yu, K., Zhu, L., et al. (2015). Sources, seasonality, and trends of southeast US aerosol: an integrated analysis of surface, aircraft, and satellite observations with the GEOS-Chem chemical transport model. *Atmospheric Chemistry and Physics*, *15*, 10,411–10,433.

Kimmel, J. R., Farmer, D. K., Cubison, M. J., Sueper, D., Tanner, C., Nemitz, E., et al. (2011). Real-time aerosol mass spectrometry with millisecond resolution. *International Journal of Mass Spectrometry*, *303*(1), 15–26. https://doi.org/10.1016/j.ijms.2010.12.004

Lee, B. H., Lopez-Hilfiker, F. D., Mohr, C., Kurten, T., Worsnop, D. R., & Thornton, J. A. (2014). An iodide-adduct high-resolution time-of-flight chemical-ionization mass spectrometer: Application to atmospheric inorganic and organic compounds. *Environmental Science & Technology*, *48*(11), 6309–6317. https://doi.org/10.1021/es500362a

Lee, T., Sullivan, A. P., Mack, L., Jimenez, J. L., Kreidenweis, S. M., Onasch, T. B., et al. (2010). Chemical smoke marker emissions during flaming and smoldering phases of laboratory open burning of wildland fuels. *Aerosol Research Letters*, *44*, i–v.

Lopez-Hilfiker, F. D., Constantin, K., Kercher, J. P., & Thornton, J. A. (2012). Temperature dependent halogen activation by N_2O_5 reactions on halide-doped ice surfaces. *Atmospheric Chemistry and Physics*, *12*(11), 5237–5247. https://doi.org/10.5194/acp-12-5237-2012

Lopez-Hilfiker, F. D., Mohr, C., D'Ambro, E. L., Lutz, A., Riedel, T. P., Gaston, C. J., et al. (2016). Molecular composition and volatility of organic aerosol in the southeastern U.S.: Implications for IEPOX derived SOA. *Environmental Science & Technology*, *50*, 2200–2209. https://doi.org/10.1021/acs.est.5b04769

Mao, J., Jacob, D. J., Evans, M. J., Olson, J. R., Ren, X., Brune, W. H., et al. (2010). Chemistry of hydrogen oxide radicals (HO_x) in the Arctic troposphere in spring. *Atmospheric Chemistry and Physics*, *10*, 5823–5838. https://doi.org/10.5194/acp-10-5823-2010

Marple, V. A., Rubow, K. L., & Behm, S. M. (1991). A microorifice uniform deposit impactor (MOUDI): Description, calibration, and use. *Aerosol Science and Technology*, *14*(4), 434–446. https://doi.org/10.1080/02786829108959504

Moharreri, A., Craig, L., Dubey, P., Rogers, D. C., & Dhaniyala, S. (2014). Aircraft testing of the new Blunt-body Aerosol Sampler (BASE). *Atmospheric Measurement Techniques*, *7*(9), 3085–3093. https://doi.org/10.5194/amt-7-3085-2014

Mohr, C., Huffman, J. A., Cubison, M. J., Aiken, A. C., Docherty, K. S., Kimmel, J. R., et al. (2009). Characterization of primary organic aerosol emissions from meat cooking, trash burning, and motor vehicles with high-resolution aerosol mass spectrometry and comparison with ambient and chamber observations. *Environmental Science & Technology*, *43*(7), 2443–2449. https://doi.org/10.1021/es8011518

Mohr, C., Richter, R., DeCarlo, P. F., Prévôt, A. S. H., & Baltensperger, U. (2011). Spatial variation of chemical composition and sources of submicron aerosol in Zurich during wintertime using mobile aerosol mass spectrometer data. *Atmospheric Chemistry and Physics*, *11*(15), 7465–7482. https://doi.org/10.5194/acp-11-7465-2011

Molod, A., Takacs, L., Suarez, M., & Bacmeister, J. (2015). Development of the GEOS-5 atmospheric general circulation model: Evolution from MERRA to MERRA2. *Geoscientific Model Development*, *8*(5), 1339–1356. https://doi.org/10.5194/gmd-8-1339-2015

Mudway, I. S., Duggan, S. T., Venkataraman, C., Habib, G., Kelly, F. J., & Grigg, J. (2005). Combustion of dried animal dung as biofuel results in the generation of highly redox active fine particulates. *Particle and Fibre Toxicology*, *2*(1), 6. https://doi.org/10.1186/1743-8977-2-6

Orsini, D. A., Ma, Y., Sullivan, A., Sierau, B., Baumann, K., & Weber, R. J. (2003). Refinements to the particle-into-liquid sampler (PILS) for ground and airborne measurements of water-soluble aerosol composition. *Atmospheric Environment*, *37*(9-10), 1243–1259. https://doi.org/10.1016/S1352-2310(02)01015-4

Ortega, A. M., Day, D. A., Cubison, M. J., Brune, W. H., Bon, D., de Gouw, J. A., & Jimenez, J. L. (2013). Secondary organic aerosol formation and primary organic aerosol oxidation from biomass-burning smoke in a flow reactor during FLAME-3. *Atmospheric Chemistry and Physics*, *13*(22), 11,551–11,571. https://doi.org/10.5194/acp-13-11551-2013

Parrella, J. P., Jacob, D. J., Liang, Q., Zhang, Y., Mickley, L. J., Miller, B., et al. (2012). Tropospheric bromine chemistry: Implications for present and pre-industrial ozone and mercury. *Atmospheric Chemistry and Physics*, *12*(15), 6723–6740. https://doi.org/10.5194/acp-12-6723-2012

Pechony, O., & Shindell, D. T. (2010). Driving forces of global wildfires over the past millennium and the forthcoming century. *Proceedings of the National Academy of Sciences*, *107*(45), 19,167–19,170. https://doi.org/10.1073/pnas.1003669107

Puxbaum, H., Caseiro, A., Sánchez-Ochoa, A., Kasper-Giebl, A., Claeys, M., Gelencsér, A., et al. (2007). Levoglucosan levels at background sites in Europe for assessing the impact of biomass combustion on the European aerosol background. *Journal of Geophysical Research*, *112*, D23S05. https://doi.org/10.1029/2006JD008114

Rienecker, M. M., Suarez, M. J., Todling, R., Bacmeister, J., Takacs, L., Liu, H.-C., et al. (2008). The GEOS-5 data assimilation system—Documentation of versions 5.0.1, 5.1.0, and 5.2.0, NASA Tech. Rep. TM-2008–104606, 27. Retrieved from https://gmao.gsfc.nasa.gov/pubs/doc/Rienecker369.pdf

Rinehart, L. R., Fujita, E. M., Chow, J. C., Magliano, K., & Zielinska, B. (2006). Spatial distribution of $PM_{2.5}$ associated organic compounds in central California. *Atmospheric Environment*, *40*, 290–303.

Roberts, J. M., Veres, P., Warneke, C., Neuman, J. A., Washenfelder, R. A., Brown, S. S., et al. (2010). Measurement of HONO, HNCO, and other inorganic acids by negative-ion proton-transfer chemical-ionization mass spectrometry (NI-PIT-MS): Application to biomass burning emissions. *Atmospheric Measurement Techniques*, *3*(4), 981–990. https://doi.org/10.5194/amt-3-981-2010

Roberts, J. M., Veres, P. R., Cochran, A. K., Warneke, C., Burling, I. R., Yokelson, R. J., et al. (2011). Isocyanic acid in the atmosphere and its possible link to smoke-related health effects. *Proceedings of the National Academy of Sciences*, *108*(22), 8966–8971. https://doi.org/10.1073/pnas.1103352108

Rolph, G. D. (2016). Real-time Environmental Applications and Display sYstem (READY) website. Silver Spring, MD: NOAA Air Resources Laboratory. Retrieved from http://www.arl.noaa.gov/ready/hysplit4.html (last access: 31 May 2016).

Schauer, J. J., & Cass, G. R. (2000). Source apportionment of wintertime gas-phase and particle-phase air pollutants using organic compounds as tracers. *Environmental Science & Technology*, *34*(9), 1821–1832. https://doi.org/10.1021/es981312t

Schauer, J. J., Rogge, W. F., Hildemann, L. M., Mazurek, M. A., & Cass, G. R. (1996). Source apportionment of airborne particulate matter using organic compounds as tracers. *Atmospheric Environment*, *30*(22), 3837–3855. https://doi.org/10.1016/1352-2310(96)00085-4

Schroder, J. C., Campuzano-Jost, P., Day, D. A., Shah, V., Larson, K., Sommers, J. M., et al. (2018). Sources and secondary production of organic aerosols in the northeastern U.S. during WINTER. *Journal of Geophysical Research: Atmospheres*, *123*, 7771–7796. https://doi.org/10.1029/2018JD028475

Seinfeld, J. H., & Pandis, S. N. (1998). *Atmospheric chemistry and physics: From air pollution to climate change*. Hoboken, NJ: John Wiley.

Simoneit, B. R. T., Schauer, J. J., Nolte, C. G., Oros, D. R., Elias, V. O., Fraser, M. P., et al. (1999). Levoglucosan, a tracer for cellulose in biomass burning and atmospheric particles. *Atmospheric Environment*, *33*(2), 173–182. https://doi.org/10.1016/S1352-2310(98)00145-9

Simpson, I. J., Akagi, S. K., Barletta, B., Blake, N. J., Choi, Y., Diskin, G. S., et al. (2011). Boreal forest fire emissions in fresh Canadian smoke plumes: C_1-C_{10} volatile organic compounds (VOCs), CO_2, CO, NO_2, NO, HCN, and CH_3CN. *Atmospheric Chemistry and Physics*, *11*(13), 6445–6463. https://doi.org/10.5194/acp-11-6445-2011

Slusher, D. L., Huey, L. G., Tanner, D. J., Flocke, F. M., & Roberts, J. M. (2004). A thermal dissociation–chemical ionization mass spectrometry (TD-CIMS) technique for the simultaneous measurement of peroxyacyl nitrates and dinitrogen pentoxide. *Journal of Geophysical Research*, *109*, D19315. https://doi.org/10.1029/2004JD004670

Sorooshian, A., Brechtel, F. J., Ma, Y., Weber, R. J., Corless, A., Flagan, R. C., & Seinfeld, J. H. (2006). Modeling and characterization of a particle-into-liquid sampler (PILS). *Aerosol Science and Technology*, *40*(6), 396–409. https://doi.org/10.1080/02786820600632282

Stith, J. L., Ramanathan, V., Cooper, W. A., Roberts, G. C., DeMott, P. J., Carmichael, G., et al. (2009). An overview of aircraft observations from the Pacific Dust Experiment campaign. *Journal of Geophysical Research*, *114*, D05207. https://doi.org/10.1029/2008JD010924

Streets, D. G., Yan, F., Chin, M., Diehl, T., Mahowald, N., Schultz, M., et al. (2009). Anthropogenic and natural contributions to regional trends in aerosol optical depth, 1980–2006. *Journal of Geophysical Research*, *114*, D00D18. https://doi.org/10.1029/2008JD011624

Sullivan, A. P., Frank, N., Kenski, D. M., & Collett, J. L., Jr. (2011). Application of high-performance anion-exchange chromatography-pulsed amperometric detection for measuring carbohydrates in routine daily filter samples collected by a national network: 2. Examination of sugar alcohols/polyols, sugars, and anhydrosugars in the Upper Midwest. *Journal of Geophysical Research*, *116*, D08303. https://doi.org/10.1029/2010JD014169

Sullivan, A. P., Frank, N., Onstad, G., Simpson, C. D., & Collett, J. L., Jr. (2011). Application of high-performance anion-exchange chromatography-pulsed amperometric detection for measuring carbohydrates in routine daily filter samples collected by a national network: 1. Determination of the impact of biomass burning in the Upper Midwest. *Journal of Geophysical Research*, *116*, D08302. https://doi.org/10.1029/2010JD014166

Sullivan, A. P., Holden, A. S., Patterson, L. A., McMeeking, G. R., Kreidenweis, S. M., Malm, W. C., et al. (2008). A method for smoke marker measurements and its potential application for determining the contribution of biomass burning from wildfires and prescribed fires to ambient $PM_{2.5}$ organic carbon. *Journal of Geophysical Research*, *113*, D22302. https://doi.org/10.1029/2008JD010216

Sullivan, A. P., May, A. A., Lee, T., McMeeking, G. R., Kreidenweis, S. M., Akagi, S. K., et al. (2014). Airborne-based source smoke marker ratios from prescribed burning. *Atmospheric Chemistry and Physics*, *14*(19), 10,535–10,545. https://doi.org/10.5194/acp-14-10535-2014

Torres-Duque, C., Maldonado, D., Pérez-Padilla, R., Ezzati, M., & Viegi, G. (2008). Biomass fuels and respiratory diseases: A review of the evidence. *Proceedings of the American Thoracic Society*, *5*(5), 577–590. https://doi.org/10.1513/pats.200707-100RP

Travis, K. R., Jacob, D. J., Fisher, J. A., Kim, P. S., Marais, E. A., Zhu, L., et al. (2016). Why do models overestimate surface ozone in the Southeast United States? *Atmospheric Chemistry and Physics*, *16*(21), 13,561–13,577. https://doi.org/10.5194/acp-16-13561-2016

Verma, V., Fang, T., Guo, H., King, L., Bates, J. T., Peltier, R. E., et al. (2014). Reactive oxygen species associated with water-soluble $PM_{2.5}$ in the southeastern United States: Spatiotemporal trends and source apportionment. *Atmospheric Chemistry and Physics*, *14*, 12,915–12,930. https://doi.org/10.5194/acp-14-12915-2014

Ward, D. E., Setzer, A. W., Kaufman, Y. J., & Rasmussen, R. A. (1991). Characteristics of smoke emissions from biomass fires of the Amazon region-BASE-A experiment. In J. S. Levine (Ed.), *Global biomass burning: Atmospheric, climatic, and biospheric implications* (pp. 394–402). Cambridge, MA: MIT Press.

Wegesser, T. C., Pinkerton, K. E., & Last, J. A. (2009). California wildfires of 2008: Coarse and fine particulate matter toxicity. *Environmental Health Perspectives*, *117*(6), 893–897. https://doi.org/10.1289/ehp.0800166

Zhang, X., Hecobian, A., Zheng, M., Frank, N. H., & Weber, R. J. (2010). Biomass burning impact on $PM_{2.5}$ over the southeastern US during 2007: Integrating chemically speciated FRM filter measurements, MODIS fire counts and PMF analysis. *Atmospheric Chemistry and Physics*, *10*, 6839–6853. https://doi.org/10.5194/acp-10-6839-2010

Zheng, M., Cass, G. R., Schauer, J. J., & Edgerton, E. S. (2002). Source apportionment of $PM_{2.5}$ in the southeastern United States using solvent-extractable organic compounds as tracers. *Environmental Science & Technology*, *36*, 2361–2371.